Surgical and Radiologic Anatomy (2019) 41:477–483
https://doi.org/10.1007/s00276-019-02200-3

ORIGINAL ARTICLE

Prevalence of anatomical variants in the clivus: fossa navicularis magna, canalis basilaris medianus, and craniopharyngeal canal

Seval Bayrak[1] · Duygu Göller Bulut[1] · Kaan Orhan[2,3]

Received: 16 November 2018 / Accepted: 31 January 2019 / Published online: 6 February 2019

Abstract

Purpose This study determined the prevalence of fossa navicularis magna (FNM), canalis basilaris medianus (CBM), and craniopharyngeal canal (CPC), the size of FNMs, and types of CBM using 3D computed tomography (CT) images.

Methods A total of 1059 3D images [649 cone beam computed tomography (CBCT) and 410 CT] were evaluated in this study. The prevalence of FNM, CBM, and CPC, length, width, and depth of FNM, and type of CBM were assessed.

Results Overall, FNM was identified in 7.6%, CPC in 0.3%, and CBM in 2.5% of the study group. Type 2 (0.1%) and Type 6 (0.1%) are the least common CBM types. There was no significant difference between genders for depth and width measurements ($p > 0.05$), however, the length of FNM was significantly higher in males than females in CBCT images ($p = 0.02$).

Conclusion FNM, CBM, and CPC are rare anatomical variants of clivus. However, they can facilitate spread of infection to the skull base or vice-versa. These types of anatomical variations should be known by radiologists to avoid unnecessary diagnosis and treatment procedures and to distinguish anatomic variations from pathological conditions.

Keywords Canalis basilaris medianus · Clivus · Craniopharyngeal canal · Fossa navicularis magna

Introduction

The clivus is located at the mid-point of the skull base. It results from the fusion of the basisphenoidal and basiocciptal bones, which begins in the 2nd month of intrauterine life until the spheno-occipital synchondrosis ossification. The ossification completes between ages 16 and 20 years [8, 19, 26].

Fossa navicularis magna (FNM) is an anatomical variant. It is a notch-shaped bony depression defect on the inferior surface of the clivus in the basiocciput [27]. FNM was first described by Testut in 1921 and is also known as fossa navicularis, canalis basilaris medianus, fossa pharyngeal, and large pharyngeal fossa [5, 8, 21]. Two theories are proposed for FNM development: (1) a remnant of the notochord canal and (2) the expansion or remnant of emissary veins [5]. FNM is an uncommon anatomical variant [6] and serves as a tract for infection between the skull base and nasopharynx [8, 26].

A craniopharyngeal canal (CPC) is an anomaly of the clivus defined as a well-corticated midline canal extending from the roof of the nasopharynx to the floor of the sella [13]. The CPC is differentiated by spheno-occipital synchondrosis and its localization. Spheno-occipital synchondrosis is located posterior and inferior to the sella turcica. CPC formation is hypothesized to be an incomplete closure of the Rathke pouch [7, 13]. Although CPC is an uncommon anomaly, it is important for diagnosing nasopharyngeal or midline skull base lesions.

Canalis basilaris medianus (CBM) is a rare anatomical variant that describes a corticated and well-defined canal between the nasopharynx and intracranial surface of the basiocciput [8]. For the development of CBM, two hypotheses have been proposed. The CBM might either have a vascular origin due to emissary veins or form from the remnants of the notochord [8]. There are six types of CBM defined in

✉ Seval Bayrak
dtseval@hotmail.com

[1] Department of Dentomaxillofacial Radiology, Dentistry Faculty, Bolu Abant İzzet Baysal University, Gölköy, 14000 Bolu, Turkey

[2] Dentomaxillofacial Radiology Department, Dentistry Faculty, Ankara University, Ankara, Turkey

[3] OMFS IMPATH Research Group, Department of Imaging and Pathology, Faculty of Medicine, University of Leuven and Oral &Maxillofacial Surgery, University Hospitals Leuven, Leuven, Belgium

the literature, three complete types: superior, inferior, and bifurcated, and three incomplete types: a thin, long channel, superior recess, and inferior recess [8, 11]. Although CBM is considered to have no clinical importance, a few cases report that complete CBM can be associated with meningocele and recurrent meningitis [10, 17].

Computed tomography (CT) and cone beam computed tomography (CBCT) are widely used in skull base and maxillofacial imaging for different purposes. CT is the preferred imaging method for craniofacial imaging to yield accurate and reliable assessments. However, its effective dose is much higher than that of conventional imaging modalities. CBCT is a technique proposed for maxillofacial imaging during the last decade, which offers similar images (such as sagittal, coronal, and axial) as traditional CT images [20]. CBCT images can be obtained with a large field of view and have the advantage of visualizing the clivus and surrounding bony structures with a lower radiation dose [2]. However, in both CT and CBCT, the radiologists should know the anatomy of this region to avoid unnecessary examinations and to distinguish anatomic variations from pathological conditions.

The purpose of this study was to determine the prevalence of FNM, CFC, and CBM in a subgroup of the Turkish population using CT and CBCT.

Materials and methods

In this study, 1059 patient CBCT ($n=649$) and CT ($n=410$) images were used (467 male and 592 female). The age range of the study group was between 9 and 83 years. The CT and CBCT images were obtained for several reasons such as temporomandibular disorders, pre-orthodontic treatment, impacted teeth surgery, obstructive sleep apnea syndrome, and paranasal sinus imaging. Patients with a history of trauma or surgery in the midline skull base were excluded.

CBCT images were obtained using the I-CAT 3D Imaging System (Imaging Sciences International, Hatfield, PA, USA) and CT images were obtained using two CT scanners (GE Lightspeed 16 slice, GE Medical Systems, Milwaukee WI, US; Siemens Somaton Sensation, 16 slice, Siemens Medical Solutions, Erlangen, Germany) with exposure parameters as shown Tables 1 and 2.

FNM was defined in sagittal slices of CBCT and CT images as a well-defined depression area on the inferior side of the clivus (Fig. 1). The length and depth of FNM was measured from sagittal planes, whereas the width was measured from axial planes. The furthermost distance in the anteroposterior direction was measured as length whereas the deepest portion was measured as depth. The furthest distance in the mediolateral direction was measured as the width (Fig. 2). A well-defined, corticated, osseous transclival defect located in the basiocciput of the clivus was identified as CBM, which was sub classified into six types (type 1 to type 6) (Fig. 3). CPC was defined

Table 2 Distribution of patients with a fossa navicularis magna (FNM), craniopharyngeal canal (CPC), canalis basilaris medianus (CBM) according to gender

Gender	Mean age ± SD	Total number	FNM *N* (%)	CPC *N* (%)	CBM *N* (%)
Male	34.96 ± 17.58	467	34 (7.3)	1 (0.2)	14 (3)
Female	30.77 ± 16.54	592	47 (7.6)	2 (0.3)	12 (2)
Total	32.62 ± 17.12	1059	81 (7.6)	3 (0.3)	26 (2.5)

SD standard deviation, *N* number

Table 1 Scanning protocols for computed tomography (CT) and cone beam computed tomography (CBCT)

	CBCT (I-CAT)	CT (GE lightspeed 16 slice)	CT (siemens somaton sensation)
KVp	120	120	120
mA	5	120	120
FOV	9–13 × 16 mm	25 × 25	25 × 25
Voxel size	0.3 mm^3	1 × 1 × 2 mm^3	1 × 1 × 2 mm^3
Display matrix	N.A	256 × 256	256 × 256
Scan type	Volumetric	Spiral 1.0 s	Spiral 1.0 s
Silice thickness	0.3 mm	2 mm	2 mm
Table speed	N.A	6.25 s	6.25 s
Pitch	N.A	0.625:1	0.625:1
Collimation	N.A	128 × 0.6	128 × 0.6
Rotation times	4.8 s	1 s/rot	0.5 s/rot
Algorithm of reconstruction	Bone	Bone	Bone
Position of acquisition	Isotropic voxel (axial, sagital, coronal)	Axial	Axial

kVp kilovoltage, *mA* miliampere, *FOV* field of view, *s* second, *N.A* not applicable

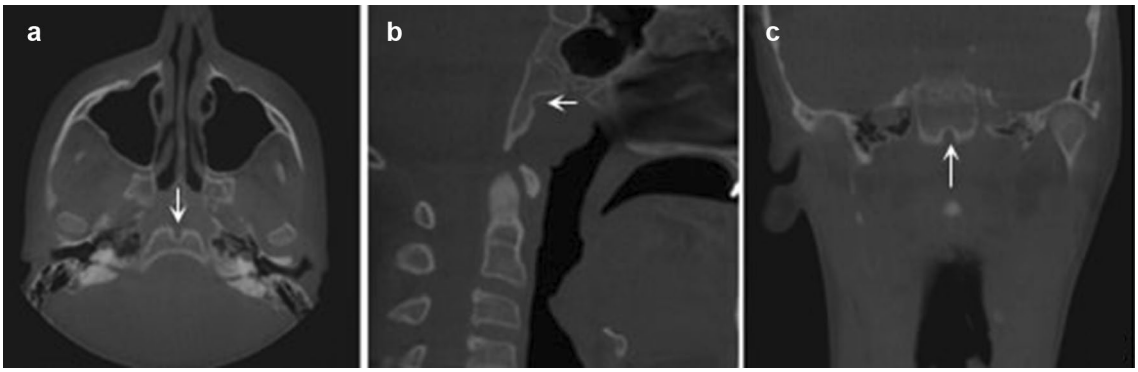

Fig. 1 White arrows show fossa navicularis magna in axial (**a**), sagittal (**b**), and coronal planes (**c**) in cone beam computed tomography (CBCT) images

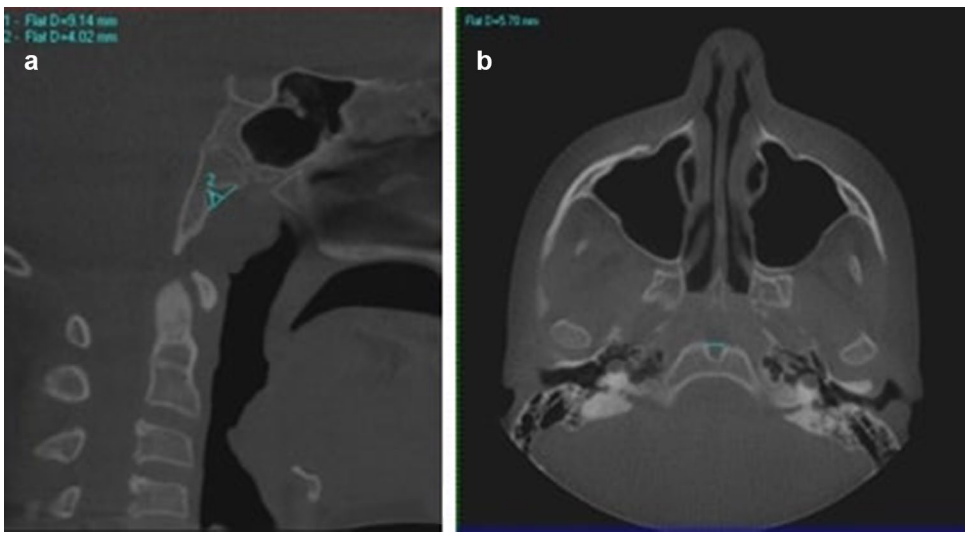

Fig. 2 Cone beam computed tomography (CBCT) images show length (1) and depth (2) measurements of fossa navicularis magna on the sagittal plane (**a**) and width measurements of fossa navicularis magna in axial planes (**b**)

as the midline corticated channel between the sella turcica and nasopharynx (Fig. 4).

Two maxillofacial radiologists evaluated all images. Observers were oriented at the beginning of the study by evaluating 20% of the images. The radiologists separately evaluated and interpreted each image twice without knowing the prevailing clinical conditions of the patients. Each condition was assessed and classified by the observers independently. When the assessments were different, the final diagnosis was obtained by repeating the evaluation and seeking consensus between the radiologists. The same observers took all measurements twice, and the mean values of all measurements were included in the statistical analysis. The observers also performed the study twice with an interval of 2 weeks to detect intra-observer variability.

Examiner reliability and statistical analysis

Statistical analyses were carried out using SPSS 20.0.1 software (SPSS, Chicago, IL, USA). Intra- and inter-examiner validation measures were conducted. To assess intra-observer reliability, the Wilcoxon matched-pairs signed rank test was used for repeat measurements. The inter-observer reliability was determined by the intraclass correlation coefficient (ICC) and the coefficient of variation (CV) [CV = (standard deviation/mean) × 100%]. Values for the ICC range from 0 to 1. ICC values greater than 0.75 show good reliability. Low CVs demonstrate the precision error as an indicator of reproducibility. Descriptive statistical methods were used. The distribution of the data normality was tested using the Shapiro–Wilk test. The differences in gender for FNM, CBM, and CPC distribution were tested using Pearson's Chi-square test and for

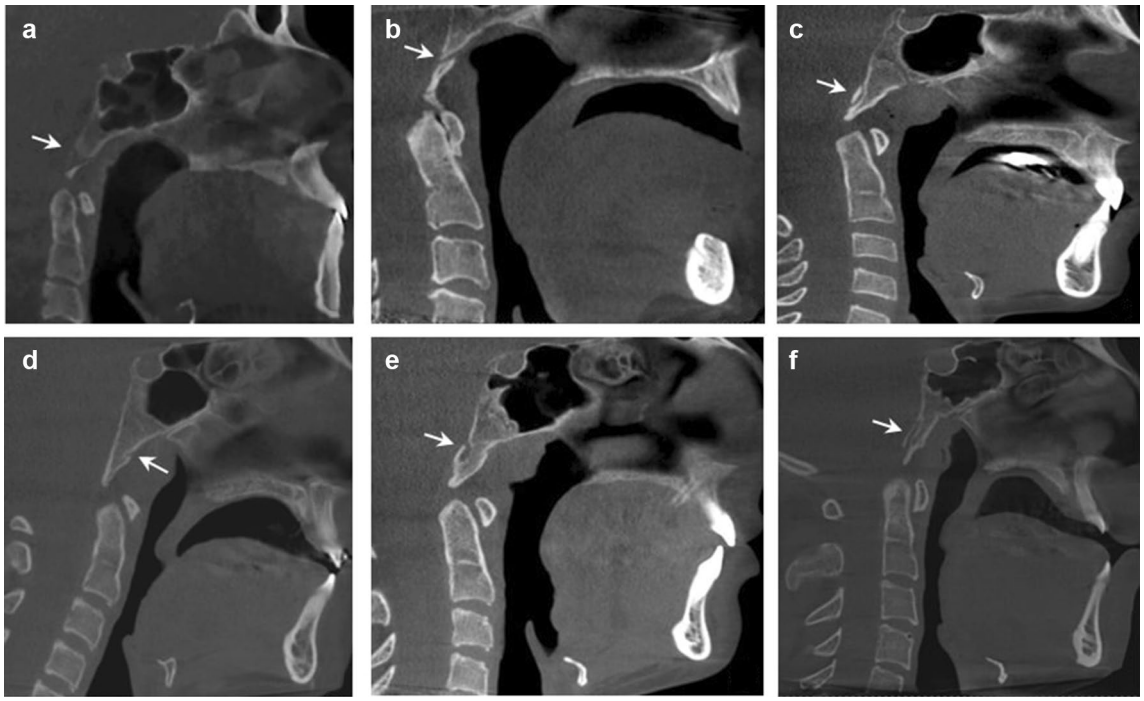

Fig. 3 White arrows show canalis basilaris medianus types: bifurcating type (**a**), inferior type (**b**), superior type (**c**), inferior recess (**d**), superior recess (**e**), and channel (**f**) in sagittal planes in cone beam computed tomography (CBCT) and CT images

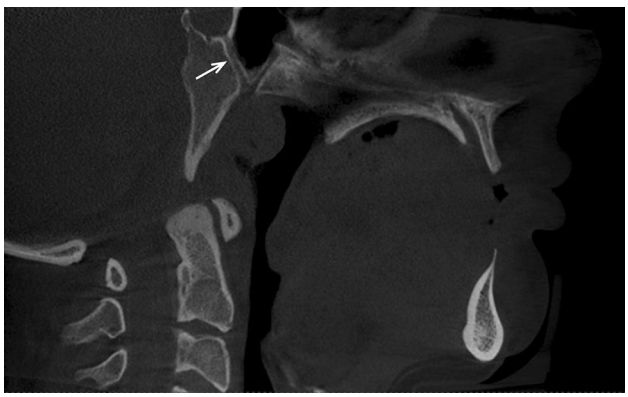

Fig. 4 White arrows show the craniopharyngeal canal in the sagittal plane in cone beam computed tomography (CBCT) images

measurements using the Student's *t* test ($p < 0.05$). Differences in measurements between age groups were tested using one-way ANOVA and post-hoc Sidak tests.

Results

Intra-observer consistency

Repeated CBCT evaluation and measurements indicated no significant intra-observer differences for both observers ($p > 0.05$). Overall intra-observer consistency for observer 1 was 88.2% and 90.4%, whereas the consistency for observer 2 was 89.2% and 92.6% between the two evaluations and measurements, respectively. All measurements were highly reproducible for both observers and no significant difference were obtained from the two measurements of the observers ($p > 0.05$).

Inter-observer consistency

The ICCs between Observer 1 and Observer 2 ranged from 0.880 to 0.900. There was a high inter-observer agreement, whereas a high ICC and low CV demonstrated that the procedure was standardized between the evaluations and measurements of the observers. No statistical differences were found among observer evaluations and measurements ($p < 0.05$). The mean of the observers was used as the final data.

Tables 1 and 2 shows the descriptive statistical data of the study population and the frequency of FNM, CPC, and CBM. The mean age of males and females was 34.96 and 30.77 years, respectively. The prevalence of FNM was 7.6% ($n = 81$) in the study group: 59 were found using CBCT (9.0%, 59/649) and 23 using CT images (5.6%, 23/410). The prevalence of CPC was 0.3% and CBM was 2.5%. There was no significant difference between genders in the distribution of FNM, CPC, and CBM ($p > 0.05$).

Table 3 shows the distribution of CBM types by gender. Type 2 (0.1%) and type 6 (0.1%) were the least common types. On the other hand, types 1, 3, and 5 were equal ($n=7$, 0.7%).

The depth, length, and width measurements of FNM are shown in Table 4 according to gender. There was no significant difference between the genders for depth and width measurements both in CBCT and CT measurements ($p>0.05$). However, the length of FNM was significantly higher in males than females in CBCT images ($p=0.02$). The length of FNM was also evaluated separately according to age group. The length (4.48 ± 1.27 mm) in the third group (30–39) was significantly smaller than the first, fourth, and fifth groups ($p=0.001$) (Table 5).

Table 3 Distribution of canalis basilaris medianus according to types and gender

Gender	Type of canalis basilaris medianus					
	Type 1 *N* (%)	Type 2 *N* (%)	Type 3 *N* (%)	Type 4 *N* (%)	Type 5 *N* (%)	Type 6 *N* (%)
Male	3 (0.6)	1 (0.2)	6 (1.3)	1 (0.2)	2 (0.4)	1 (0.2)
Female	4 (0.7)	–	1 (0.2)	2 (0.3)	5 (0.8)	–
Total	7 (0.7)	1 (0.1)	7 (0.7)	3 (0.3)	7 (0.7)	1 (0.1)

N number

Table 4 Comparison of the depth, length and width measurements of fossa navicularis magna according to gender on CBCT and CT

Gender	Depth (mm)			Length (mm)			Width (mm)		
	Min–Max	Mean ± SD	*P* value	Min–Max	Mean ± SD	*P* value	Min–Max	Mean ± SD	*P* value
CBCT measurements									
Male ($n=21$)	1.62–5.66	2.94 ± 0.99	0.35	3.61–11.19	7.86 ± 1.88	0.02*	2.10–7.80	5.41 ± 1.50	0.51
Female ($n=38$)	1.50–6.90	2.66 ± 1.14		2.66–10.30	6.76 ± 1.65		1.70–8.11	5.13 ± 1.62	
Total ($n=59$)	1.50–6.90	2.76 ± 1.09		2.66–11.19	7.15–1.80		1.70–8.11	5.23 ± 1.57	
CT measurements									
Male ($n=13$)	3.49–4.94	4.20 ± 0.55	0.75	3.50–4.91	4.14 ± 0.55	0.82	3.53–4.80	4.10 ± 0.49	0.79
Female ($n=9$)	3.51–4.88	4.12 ± 0.54		3.56–4.86	4.08 ± 0.50		3.64–4.84	4.05 ± 0.48	
Total ($n=22$)	3.49–4.94	4.17 ± 0.54		3.50–4.91	4.12 ± 0.52		3.53–4.84	4.08 ± 0.47	

SD standard deviation

*Statistically significant level is $p<0.05$

Table 5 Comparison of the depth, length and width measurements of fossa navicularis magna according to age groups

	Age groups					
	1. Group 10–19 years ($N=24$)	2. Group 20–29 years ($N=28$)	3. Group 30–39 years ($N=13$)	4. Group 40–49 years ($N=13$)	5. Group >50 years ($N=10$)	*P* value
Depth (mm)						
Min–Max	1.75–6.90	1.50–4.85	2.12–5.66	1.50–4.87	1.90–5.16	0.102
Mean ± SD	3.14 ± 1.24	2.96 ± 1.07	3.81 ± 0.98	2.38 ± 1.26	3.26 ± 1.08	
Length (mm)						
Min–Max	2.66–10.12	3.50–10.87	3.60–7.60	4.84–8.58	4.74–11.17	0.001*
Mean ± SD	$7.05\pm1.76^{+}$	$5.99\pm2.16^{*+-}$	4.48 ± 1.27*	$7.15\pm1.52^{+-}$	$7.44\pm2.04^{+-}$	
Width (mm)						
Min–Max	1.90–8.11	2.10–7.80	3.00–6.25	3.60–6.60	1.70–6.60	0.139
Mean ± SD	5.16 ± 1.79	5.08 ± 1.37	4.05 ± 0.82	5.50 ± 1.10	4.65 ± 1.34	

Different superscript symbols indicate a significant difference between groups

n number

*Statistically significant level is $p<0.05$

Discussion

FNM is close to the nasopharynx, clivus, and sphenoid sinuses. Therefore, in the differential diagnosis of this anatomical variation, several conditions should be assessed: local or metastatic tumors, adenoid retention cyst, adenoid hypertrophy, Rathke pouch cyst, Tornwaldt cyst, sphenoidal sinus mucocele, and dermoid teratoma of the posterior nasopharyngeal wall [6]. It is important to know the anatomy of the bone variations in this region because various pathological lesions can mimic the anatomy or vice-versa.

Several previous studies evaluate these anatomical variations on dry skulls using CT and CBCT images. In a previous study by Rossi [25], FNM was reported in 55 (1.5%) of 3712 skulls. Romiti reported 9 (0.9%) cases in a 990 dry skull series [24]. In a similar study, 7 (2.1%) FNM cases were found in 335 skulls by Rizzo [23] and in 3 (1.49%) out of 202 skulls by Ray et al. [22]. Cankal et al. [6] found FNM in 26 (5.3%) of the 492 dry skulls and in 16 (3%) of 525 CT scans in the Turkish population. Ersan [9] examined a series of CBCT images from 732 patients and reported the prevalence of FNM as 6.6%. In this study, the prevalence of FNM was 7.6%, which is higher than the previous studies. This may due to different populations and methodologies. However, our results are in line with Ersan's [9], who studied the same population and used the same imaging modality as CBCT.

Previous studies indicated an FNM length of 7–13 mm, width of 6–8 mm, and depth of 2–5.5 mm [5]. Cankal et al. [6] reported FNM depth as 2.24 mm, width as 2.85 mm, and length as 5.12 mm using a digital micrometer. Ersan [9] reported a depth of 2.2 mm, length of 5.8 mm, and width of 4.7 mm in CBCT measurements. In the present study, depth was 2.76 mm and 4.17 mm, length 7.15 mm and 4.12 mm, and width 5.23 mm and 4.08 mm in CBCT and CT measurements, respectively. Ersan [9] reported that there was no difference in the size of FNM between age groups. However, in the current study, the length in the 30–39 year age group was smaller than in the others.

Arey evaluated 100 patients from infancy to 8 months old, observed a ratio of 10% CPC in all live births, and reviewed the autopsy data of 11 previous studies. The estimated incidence was 0.42% and the majority of the cases were adult [4]. Abele et al. [1] retrospectively analyzed 29 cases of CPC with CT. Although there are a few case reports and anatomic studies about CPC in the literature, there is insufficient data on its prevalence [12]. In this study, only three patients (0.3%) had CPC, suggesting a low incidence in this particular population, which may be due to the low number of pediatric patients in our study group. However, further studies should be done with a wide age range and a larger sample group, especially pediatric patients.

CBM is generally considered an anatomical variant with no clinical significance [14]. The prevalence of CBM reported in the literature is 4–5% in children and 2–3% for adults [28]. However, some studies report CBM can serve as a potential pathway for disease progression, such as meningitis. Hemphill et al. [10] and Martinez et al. [17] report a CBM that was associated with a meningocele causing recurrent meningitis. Jacquemin et al. [11] presented a case of CBM with atypical bacterial meningitis. Lohman et al. [16] also reported a single case of CBM associated with a Tornwaldt cyst. Syed et al. [28] reported two cases of CBM, using CBCT imaging. In both cases, the formation of CBM was not associated with meningitis or other problems. In this study, the age range of patients with CBM was 15–75 years and the CBM prevalence was 2.5, which is consistent with the literature. Types 1, 3, and 5 were the most common. Because there is no study evaluating the prevalence of CBM types in the literature, no comparison can be made. Moreover, the pathology caused by CBMs could not be evaluated due to the retrospective nature of our study.

The clinical relevance of these anatomical variations is important, because these variations can be misinterpreted as pathology or vice-versa. In a case report by Prabhu et al. [21], FNM was defined intermittent fever, neck pain, and neck stiffness and diagnosed as clival osteomyelitis in a 5 year old girl. In another report, Segal et al. [26] noticed FNM in a 12 year old girl referred for headache, fever, and neck stiffness. In both case reports, it was concluded that the infections spread intracranially via FNM. Similarly, Akyel et al. [3] stated that although CPC is a rare anomaly, it should be diagnosed correctly because it can cause iatrogenic hypopituitarism and cerebrospinal fluid leakage. In addition, meningocele, craniopharyngioma, glioma, dermoid, teratoma, adenoma, and pituitary gland dysfunction are associated with CPC [1, 15, 20]. Various rare conditions can also be associated with the presence of CBM. Khairyet et al. [14] reported the development of meningitis due to a block in a cerebrospinal fluid leak via CBM. Lohman et al. [16] and Morabito et al. [18] presented Tornwaldt's and pharyngeal enterogenous cysts associated with CBM in a 45 year old male patient and a newborn, respectively.

Conclusion

In conclusion, although the prevalence of these anatomic variations is low, they may cause the spread of nasopharyngeal infections to the skull base. The radiologist may encounter these anatomic structures during radiographic examination, so the presence of these structures and their radiographic characteristics should be known; otherwise, it may suggest a pathological condition and may lead to unnecessary diagnosis and treatment procedures.

Author contributions Protocol Development: KO. Data Collection-Analysis: SB, KO. Manuscript Writing: DGB, SB. Manuscript Editing: KO.

Compliance with ethical standards

Conflict of interest The authors declare that there is no conflict of interest.

References

1. Abele TA, Salzman KL, Harnsberger HR, Glastonbury CM (2014) Craniopharyngeal canal and its spectrum of pathology. Am J Neuroradiol 35:772–777
2. Ahmad M, Jenny J, Downie M (2012) Application of cone beam computed tomography in oral and maxillofacial surgery. Aust Dent J 57(Suppl 1):82–94
3. Akyel NG, Alimli AG, Demirkan TH, Sivri M (2018) Persistent craniopharyngeal canal, bilateral microphthalmia with colobomatous cysts, ectopic adenohypophysis with Rathke cleft cyst, and ectopic neurohypophysis: case report and review of the literature. Childs Nerv Syst 34:1407–1410
4. Arey LB (1950) The craniopharyngeal canal reviewed and reinterpreted. Anat Rec 106:1–16
5. Beltramello A, Puppini G, El-Dalati G, Girelli M, Cerini R, Sbarbati A et al (1998) fossa navicularis magna. Am J Neuroradiol 19:1796–1798
6. Cankal F, Ugur HC, Tekdemir I, Elhan A, Karahan T, Sevim A (2004) Fossa navicularis: anatomic variation at the skull base. Clin Anat 17:118–122
7. Cho KH, Chang H, Yamamoto M, Abe H, Rodriguez-Vazquez JF, Murakami G et al (2013) Rathke's pouch remnant and its regression process in the prenatal period. Childs Nerv Syst 29:761–769
8. Currarino G (1988) Canalis basilaris medianus and related defects of the basiocciput. Am J Neuroradiol 9:208–211
9. Ersan N (2017) Prevalence and morphometric features of fossa navicularis on cone beam computed tomography in Turkish population. Folia Morphol (Warsz) 76:715–719
10. Hemphill M, Freeman JM, Martinez CR, Nager GT, Long DM, Crumrine P (1982) A new, treatable source of recurrent meningitis: basioccipital meningocele. Pediatrics 70:941–943
11. Jacquemin C, Bosley TM, al Saleh M, Mullaney P (2000) Canalis basilaris medianus: MRI. Neuroradiology 42:121–123
12. Kasim N, Choudhri A, Alemzadeh R (2018) Craniopharyngeal canal, morning glory disc anomaly and hypopituitarism: what do they have in common? Oxf Med Case Rep 2018:018
13. Kaushik C, Ramakrishnaiah R, Angtuaco EJ (2010) Ectopic pituitary adenoma in persistent craniopharyngeal canal: case report and literature review. J Comput Assist Tomogr 34:612–614
14. Khairy S, Almubarak AO, Aloraidi A, Alahmadi KOA (2017) Canalis basalis medianus with cerebrospinal fluid leak: rare presentation and literature review. Br J Neurosurg. https://doi.org/10.1080/02688697.2017.1346173
15. Kizilkilic O, Yalcin O, Yildirim T, Sener L, Parmaksiz G, Erdogan B (2005) Hypothalamic hamartoma associated with a craniopharyngeal canal. Am J Neuroradiol 26:65–67
16. Lohman BD, Sarikaya B, McKinney AM, Hadi M (2011) Not the typical Tornwaldt's cyst this time? A nasopharyngeal cyst associated with canalis basilaris medianus. Br J Radiol 84:169–171
17. Martinez CR, Hemphill JM, Hodges FJ III, Gayler BW, Nager GT, Long DM et al (1981) Basioccipital meningocele. Am J Neuroradiol 2:100–102
18. Morabito R, Longo M, Rossi A, Nozza P, Granata F (2013) Pharyngeal enterogenous cyst associated with canalis basilaris medianus in a newborn. Pediatr Radiol 43:512–515
19. Neelakantan A, Rana AK (2014) Benign and malignant diseases of the clivus. Clin Radiol 69:1295–1303
20. Pinilla-Arias D, Hinojosa J, Esparza J, Munoz A (2009) Recurrent meningitis and persistence of craniopharyngeal canal: case report. Neurocirugia (Astur) 20:50–53
21. Prabhu SP, Zinkus T, Cheng AG, Rahbar R (2009) Clival osteomyelitis resulting from spread of infection through the fossa navicularis magna in a child. Pediatr Radiol 39:995–998
22. Ray B, Kalthur S, Kumar B, Bhat M, D'souza A, Gulati H et al (2014) Morphological variations in the basioccipital region of the South Indian skull. Nepal J Med Sci 3:124–128
23. Rizzo A (1901) Canale cranio faringeo, fossetta faringea, interparietali e pre-interparietali nel cranio umano. Mon Zool Ital 12:241–252
24. Romiti G (1890) La fossetta faringea nell'osso occipitale dell'uomo. Atti Soc Toscana Sci Nat 1:11
25. Rossi U (1891) Il canale cranio-faringeo e la fossetta faringea. Monitore Zoologico Italiano 2:117
26. Segal N, Atamne E, Shelef I, Zamir S, Landau D (2013) Intracranial infection caused by spreading through the fossa naviclaris magna—a case report and review of the literature. Int J Pediatr Otorhinolaryngol 77:1919–1921
27. Syed AZ, Mupparapu M (2016) Fossa navicularis magna detection on cone-beam computed tomography. Imaging Sci Dent 46:47–51
28. Syed AZ, Zahedpasha S, Rathore SA, Mupparapu M (2016) Evaluation of canalis basilaris medianus using cone-beam computed tomography. Imaging Sci Dent 46:141–144